DOI: 10.51975/VEWJ4581
Journal of the Nigerian Society of Chemical Engineers, 36(1), 2021

MIL-53(FE) / COW BONE CHAR COMPOSITE FOR CHROMIUM REMOVAL FROM TANNERY WASTEWATER

***Ajayi O. A.[1], Nanbyen S.[1]. Oladipo A.A.[2] and Nwafulugo, F. U.[3]**
[1]Department of Chemical Engineering, Ahmadu Bello University, Zaria. Kaduna State.
[2]Department of Environmental Engineering, Cyprus Science University, Girne, TRCN Mercin 10, Turkey.
[3]Federal Polytechnic, Oko, Anambra State, Nigeria**Corresponding Author:** segeaj@gmail.com

ABSTRACT

MIL-53(Fe)/Cow bone char composite, prepared via the sol-gel method was used for the removal of chromium from real tannery effluent having an initial concentration of 40mg/l. The characteristics of MIL-53(Fe)/Cow bone char were studied using X-ray diffraction (XRD), Fourier transform infrared spectroscopy (FTIR), thermo gravimetric analysis (TGA) Boehm titration and scanning electron microscopy (SEM-EDX). Adsorption capacity of MIL-53(Fe)/Cow bone char composite for chromium was 19.61 mg/g with a removal efficiency of 87.8% at an optimal bed height of 2.4cm (2.0g) for MIL-53(Fe)/Cow bone char composite, time of 2 minutes and pH_{pzc}=5.4.The kinetic studies showed that the adsorption data were well fitted to the pseudo second-order model with high correlation coefficient R^2=0.9911. Furthermore, the adsorption isotherm equilibrium studies confirmed that the Langmuir model best described the adsorption process of chromium onto MIL-53(Fe)/Cow bone char composite. Analysis of data with Dubinin–Radushkevich and Temkin isotherms showed that adsorption of chromium onto MIL-53(Fe)/Cow bone char composite is physical in nature.

1. INTRODUCTION

Wastewater discharge from industrial sectors such as agriculture, textile, tanneries, pulp and paper contribute largely to environmental pollution when untreated. It may contain heavy metals like cadmium and chromium that are toxic, mutagenic, carcinogenic and cause hormonal disorder to human life.

Tannery waste is generated in huge amount during the tanning process by leather industries all over the world (Mohammed *et al*., 2017). The used and non-useable hides and skins along with the excess chemicals and water used in the process constitute solid and liquid wastes in the tannery (Mohammed *et al*., 2017), which when untreated affect streams, groundwater, land and sewers in which they are discharged. Important pollutants associated with the tanning industry include chlorides, tannins, chromium, sulphate, sulphides and increasing use of synthetic chemicals such as pesticides, dyes and finishing agents.

Several adsorbents have been investigated including zeolite, cow bone, activated carbon, banana peel, sugarcane bagasse, rice husk, palm kernel shell, coconut shell etc. Modern technology employs the use of composites that have extraordinary combination of properties (Araoye, 2015). One of the materials used are the metal organic framework (MOFs) with carbon-based materials.

Recently, metal of organic framework materials (MOFs) with high porosity and high surface area have gained application in adsorption, membrane separation, sensing, catalysis and proton conduction, owing to their water stable structure (Wang *et al*., 2016). They have adjustable surface properties, and have more abundant and controllable porous structures compared to conventional porous materials such as zeolite, silica and activated carbon (Jiao *et al*., 2017).

Cow bones used in this research constitutes a waste of natural resources especially in developing countries. Cow bones which are obtainable from slaughtered cows in abattoirs are readily available in Nigeria and are usually burnt or sold to feed mill for the production of animal feeds. Cow bone char consists mainly of 57–80% tricalcium phosphate,6–10% calcium carbonate and 7–10% carbon (Fawell, 2006).

The use of MIL-53(Fe)/cow bone char composite for the removal of chromium in tannery wastewater through the process of adsorption has not been harnessed and thus, will be used in this present study.

2. MATERIALS AND METHODS

2.1 Materials and Instruments

All chemical reagents, namely: Iron (III) chloride hexahydrate ($FeCl_3.6H_2O$), Terephthalic acid (H_2BDC) N,N'-Dimethylformamide (DMF, 99.8%), Ethylene glycol and Sodium hydroxide were of analytical grade

(≥98%). Cattle bones were collected at Zango abattoir, Zaria, Nigeria. Deionized water was obtained from the PTDF Laboratory, Department of Chemical Engineering Ahmadu Bello University, Zaria. Tannery wastewater was collected from the Nigerian Institute of Leather and Science Technology (NILEST), Zaria, Nigeria.

2.2 Synthesis of MIL-53(Fe)

MIL-53(Fe) powder was prepared via a modified previously reported method (Dan *et al*., 2017; Oladipo, 2018). A mixture of Iron (III) chloride hexahydrate ($FeCl_3.6H_2O$) (1.35g), 1,4-benzenedicarboxylic acid (H_2BDC) (0.83g), and N,N'-Dimethylformamide (DMF) (112 ml) were mixed and stirred at room temperature using a magnetic stirrer until it became clear, then the reaction mixture was transferred into a 100ml Teflon-lined stainless steel autoclave and heated at 180°C for 10h. After the heat treatment, the autoclave was allowed to cool to room temperature and the resultant suspension was filtered and the orange MIL-53(Fe) powder residue was washed with 200ml deionized water and allowed to dry at 150^0C in the oven for 24 hours in order to remove the DMF in the pores. The resulting sample was stored at room temperature in a covered glass container until the time of study. The functional groups, surface morphology, crystal structure and surface area were determined using FTIR spectrophotometer, SEM, XRD and BET respectively for the as-prepared MIL-53(Fe).

2.3 Preparation of bone char

Cow bone char was prepared via a previously reported method (Patel *et al*., 2015). Cattle bones collected at Zango abattoir, Zaria, Nigeria were parboiled with NaOH, washed thoroughly with water several times and dried at 100 ^oC for 1hour. The dried bones were carbonized at a temperature of 500 ^oC for a residence time of 1hour resulting into bone char. The bone char was further ground to powder using a ceramic mortar and pestle followed by sieving to a particle size of 75 µm with an electric sieve shaker.

2.4 Synthesis of MIL-53(Fe)/Cow bone char composite

The composite was prepared via a previously reported method (Oladipo, 2018). 4.2 g of the as-prepared MIL-53(Fe) was suspended into 100 ml ethylene glycol in a flask and stirred for 1hour. And then, 3.2 g of cow bone powder was added to the above suspension, followed by continuous stirring with heating for 190 mins at 100 ^oC for solvent evaporation. The resulting solid was washed severally with 160ml deionized water and 40 ml ethanol and decanted with a suction pump and sinter glass. It was further dried in the oven at 80 ^oC for 5hours and finally calcined at 500 ^oC for 1h and cooled, sieved and stored in desiccator.

2.5 Treatment of tannery wastewater by fixed-bed system

The dynamic sorption studies were carried out in a plastic column of 1.2 cm in diameter and 7.5 cm in length. Different masses of 0.5 g, 1.25 g and 2.0 g of composite was packed into the column, achieving a bed height of 0.6 cm, 1.5 cm and 2.4 cm respectively. The tannery wastewater with an initial concentration of 40 mg/l was allowed to pass over the adsorbent bed at different times of 2 mins to 16 mins. The initial and final chromium concentration in the effluent samples was determined by atomic absorption spectroscopy (SHIMADZU, Model-AA6800 AAS).The amount of heavy metal adsorbed (q_t) at any given time (t) and at equilibrium (q_e) can be expressed as Equations (1) and (2) respectively (Chowdhury *et al*., 2013; Agoyi *et al*., 2015).

$$q_t = \left(\frac{C_o - C_t}{m}\right)V \quad (1)$$

$$q_e = \left(\frac{C_o - C_e}{m}\right)V \quad (2)$$

While the percentage of heavy metal adsorbed is expressed as equation 3:

$$\% = 100\left(\frac{C_o - C_t}{C_o}\right) \quad (3)$$

Where:

C_0 is the initial chromium concentration (mg/l)

C_t is the chromium concentration at time t (mg/l)

C_e is the molar equilibrium concentration of the solute remaining after adsorption (mg/l)

M is the mass of the adsorbent (g)

V is the volume of solution used (l)

2.6 Column desorption of MIL-53(Fe)/cow bone char composite and regeneration studies

Desorption studies were performed with MIL-53(Fe)/cow bone char composite that was saturated with tannery wastewater of pre-determined chromium concentrations. The flow rate was adjusted to 5 ml/min at a bed height of 2.4 cm. After the column had reached exhaustion, the exhausted MIL-53(Fe)/cow bone char composite was regenerated using 0.05 M NaOH. After elution, the bed was washed with distilled water until the pH stabilised close to neutral (7.0). Three cycles of

sorption-desorption-regeneration were carried out to evaluate the MIL-53(Fe)/cow bone char composite capacity. The chromium removal percentage was determined in each cycle.

3. RESULTS AND DISCUSSION

3.1 Physicochemical characteristics of tannery wastewater

From Table 1, the total suspended solids concentration in the sample tannery wastewater was 5920 mg/l. Hence tannery industrial waste cannot be discharged into the environment. Similarly, total dissolved solid concentration was 7160 mg/l indicating that the tannery wastewater contain soluble solids as well as floating solids. The result of Table 1 shows a COD and BOD concentration of 1600 mg/l and 170mg/l respectively. This is due to the use of inorganic chemicals. The pH of wastewater is the strength of acidity or alkalinity of the wastewater, which is the measure of hydrogen ion concentration in the wastewater (Oke *et al*., 2006).

Table 1: Physicochemical Parameters of Tannery Wastewater

S/n	Parameter	Unit	Result
1	pH	-	6.8
2	Dissolved Oxygen (DO)	mg/l	210
3	Biological Oxygen Demand	mg/l	170
4	Total Dissolved Solids	mg/l	7160
5	Total Suspended Solids	mg/l	5920
6	Chemical Oxygen Demand	mg/l	1600
7	Total Chromium Concentration	mg/l	40
8	Electrical Conductance	µmhos/cm	190
9	Color	Hazen Unit	1200

3.2 Characterization of samples

Fig. 1 presents the XRD pattern of the synthesized MIL-53(Fe), the diffraction lines appeared at 2θ of 8.9 (101), 11.2, 14.5, 17.5 (002), 23.5 (302), were identical to those reported for standard MIL-53(Fe) (Araya *et al.*, 2017; Oladipo, 2018) and no other lines were observed indicating that the pure crystalline phase of MIL-53(Fe) was synthesized. The XRD pattern of bone char is consistent with the standard crystalline hydroxyapatite and distinct diffraction peaks were observed at the 2θ of 26.3°, 28.2°, 32.1°, 37.9°, 43.2°, 47.8°, 49.4°, 50.4° and 62° which is agrees with the JCPDS card no: 82-1943. The XRD pattern of the MIL-53 (Fe)/char exhibits the coexistence of both MIL-53 (Fe) and bone char phases, no any impurity peaks detected, and thus indicated the high purity of the composite. While the characteristic diffraction peaks of MIL-53(Fe) reduced in intensity in the composite with no shift, the retained bone char peaks became more crystalline in nature in the composite and the structure of MIL-53(Fe) remain unchanged after the deposition of CBC (Hu *et al*., 2017).

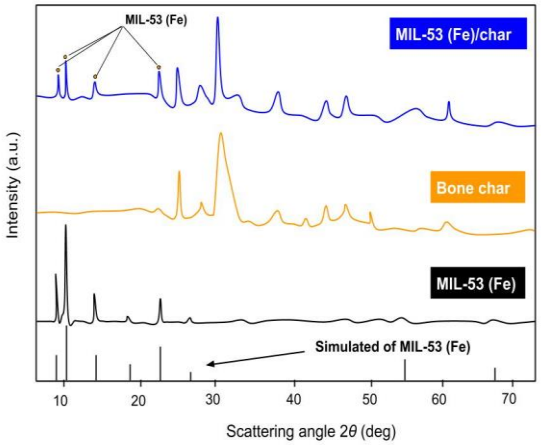

Fig. 1: XRD patterns for samples

The morphology and spectra of elemental analysis of cow bone char, MIL-53(Fe) and MIL-53(Fe)/cow bone char composite are reported in Fig.2. The micrograph for cow bone char clearly shows that the sample had undergone significant structural changes due to the thermal

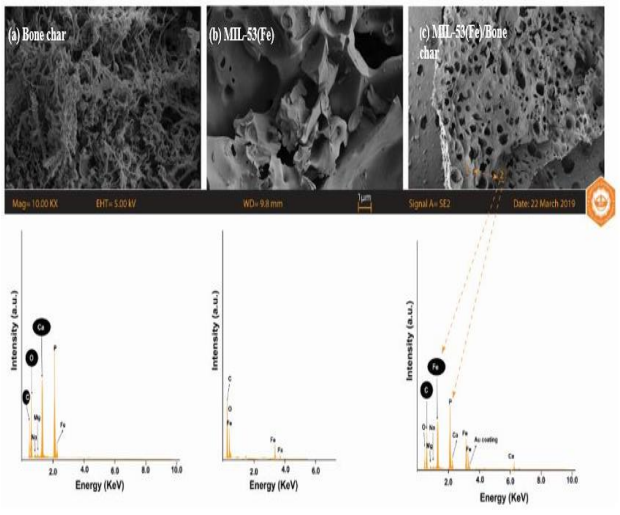

Fig. 2: SEM-EDX images for samples

treatment at 500 ºC which indicates that the thermal treatment creates more pores on the surface and increases the surface area (Mendoza-Castillo *et al*., 2014). Cow bone char exhibits a distinct morphology from the MIL-53 (Fe). As seen, the cow bone char is characterized by a highly dense continuous fibrous-like structure with crunchy textural surface and its chemical composition includes the presence of carbon, oxygen, phosphorus, and calcium, which are the main components of hydroxyapatite (Mendoza-Castillo *et al*., 2014) with minor traces of sodium, iron and magnesium. These results are consistent with the results of X-ray diffraction (see Fig. 1).

In contrast, the MIL-53 (Fe) morphology is homogeneous and characterized by well-defined smooth surface and pronounced polyhedron-like crystalline structure and its chemical composition include the presence of Iron (Fe), carbon and oxygen as depicted on the physicochemical characteristic for the sample in Table 2 as reported by Oladipo *et al*. 2017).

The surface of the MIL-53(Fe)/cow bone char is relatively smooth with heterogeneous meso and micro-pores and thick cuticle-like edges because of hetero-junctions of the pores of cow bone char onto the MIL-53(Fe) structure and the thermal treatment of the composite, which increased the porosity of the structure. Its chemical composition includes the presence of carbon, oxygen, phosphorus, calcium from the hydroxyapatite structure of cow bone char and Iron with minor traces of sodium, iron and magnesium.

The FTIR spectra are shown in Figs. 3, 4 & 5 respectively. For the MIL-53(Fe), a broad vibration at around 3480 $cm^{-1}$was attributed to the stretching vibrations of the O–H of water molecules adsorbed on the surface. The asymmetric (γ_{as}C-O) and symmetric (γ_s C-O) stretching of carboxyl group could be described by the appearance of sharp vibrations at 1525 cm^{-1} and 1380 cm^{-1} respectively indicating the presence of dicarboxylate linkers within the framework (Oladipo, 2018). The carbonyl groups (C=O) of the carboxylate ligand (COO) were visible at 1696 cm^{-1}, whereas a very sharp peak at 750 and 696 cm^{-1} corresponds to the Csp^2-H (C=C-H) bending vibrations, which belong to the benzene rings of carboxylates. The characteristic coordination bonds between Fe^{3+} cations and -OOC-C_6H_4-COO- carboxylate anions were observed at a very low wave number of 545 cm^{-1} which implies the existence of a Fe-oxo-bond present in the MIL-53(Fe) structure that exists between the carboxylic group of terephthalic acid linker and the inorganic iron(III) metal (Zhang *et al*., 2016; Oladipo, 2018). The MIL-53(Fe) spectrum clearly exhibited the characteristic absorption peaks and thus confirms the formation of MIL-53(Fe) structure (Oladipo, 2018).

For the cow bone char, the C-O stretching vibrations at 1453 with a shoulder at 1421 cm^{-1} has been assigned to CO_3^{2-} group indicating that CO_3^{2-} is present (Patel *et al*., 2015). The bands at 1041 and 962 cm^{-1} has been assigned to the P-O stretching vibrations of PO_4^{3-} group. The bands at 600, 561 and 475 cm^{-1} corresponds to PO_4^{3-} bending vibrations (Patel *et al*., 2015).

The intensity of the characteristic absorption peaks of MIL-53 (Fe) were decreased, the peak at 1380 cm^{-1} become narrower and the Fe-O band was widened at 545cm^{-1} (Oladipo, 2018). The bands at 1026 and 963 cm^{-1} is seen to also appear which is assigned to the P-O stretching vibrations of PO_4^{3-} group from the hydroxyapatite structure of the bone char. The broad vibration from the MIL-53(Fe) is seen to disappear in the spectra of the composite as a result of sintering at 500 ºC and thus, becoming broader.

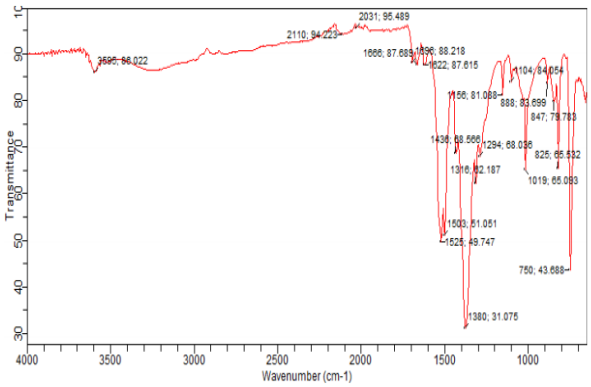

Fig. 3: FTIR for MIL-53(Fe)

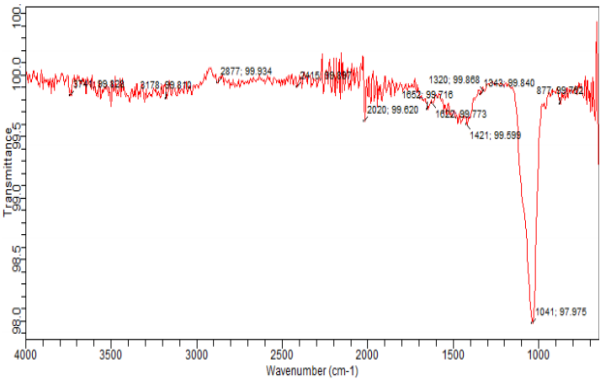

Fig. 4: FTIR for Cow bone char

DOI: 10.51975/VEWJ4581
Journal of the Nigerian Society of Chemical Engineers, 36(1), 2021

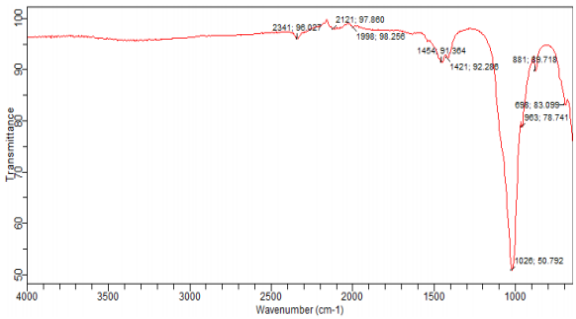

Fig. 5: FTIR for MIL-53(Fe)/Cow bone char composite

The thermal stability of MIL-53(Fe), cow bone char and MIL-53(Fe)/cow bone char composite was studied by means of TG analysis using the TG 209 F1 Libra machine at a heating rate of 10 ^{o}C/min with nitrogen gas as shown in Figures 6, 7 and 8 respectively.

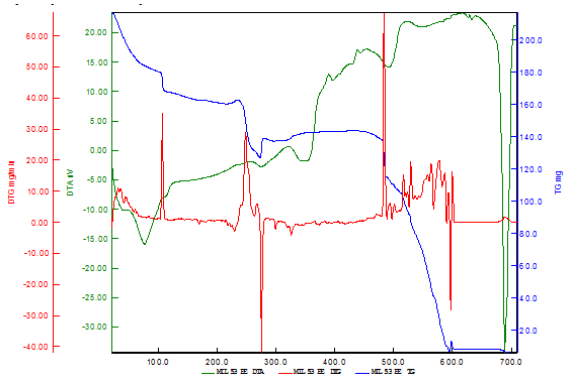

Fig. 6: DTA/TGA curves for MIL-53(Fe)

For MIL-53(Fe), the DTA/ TG profile shown in Fig.6 exhibits an endothermic peak between~90 ^{o}C to 110 ^{o}C with a minimal weight loss up to 180 mg which is as a result of evaporation of moisture from the surface of the MIL-53(Fe). The weight loss became constant from 160 mg in the temperature range of 120 ^{o}C to 280 ^{o}C which was due to free DMF occupation inside the pores. The loss was continued at the exothermic peak between 280 ^{o}C to 480 ^{o}C which can be attributed to the degradation of the organic ligand, H_2BDC. A low rate of decomposition was observed between 520 ^{o}C to 680 ^{o}C followed by a sharp decrease in weight due to complete decomposition of MIL-53(Fe).

Thermal analysis was used to investigate the high temperature behavior of cow bone char shown in Fig.7.

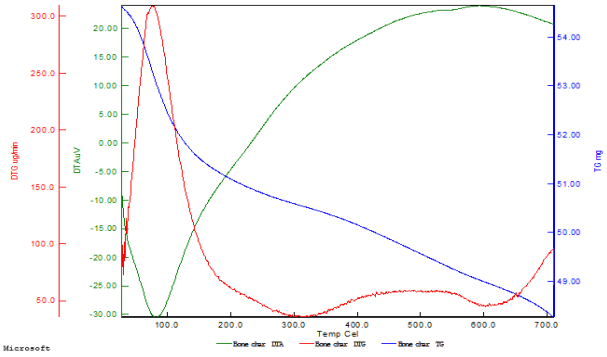

Fig. 7: DTA/TGA curves for cow bone char

The endothermic loss at 50 ^{o}C to 150 ^{o}C corresponds to the removal of absorbed moisture. The exothermic losses at 150 ^{o}C to 550 ^{o}C are attributed to the degradation of the organic substances, fats and collagen. The endothermic loss at 600 ^{o}C to 700 ^{o}C corresponds to the decomposition into calcium oxide from calcium carbonate. This result is consistent with those obtained by Patela *et al*. (2015).

Thermal analysis was used to investigate the high temperature behavior of MIL-53(Fe)/cow bone char composite as shown in Fig. 8

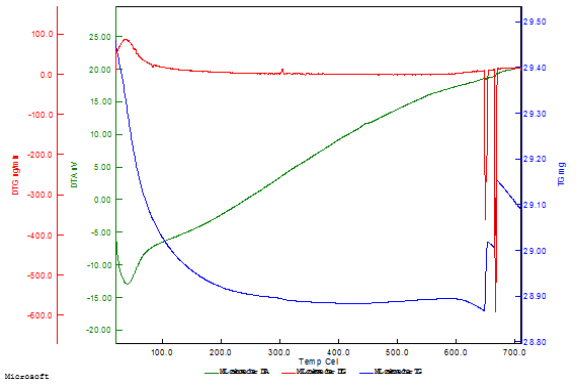

Fig. 8: DTA/TGA curves for MIL-53(Fe)/Cow bone char composite

The first endothermic peak between 50 ^{o}C to 90 ^{o}C is attributed to the evaporation of moisture from the surface of the composite as seen in the individual thermal characteristics of MIL-53(Fe) and cow bone char. The second weight loss peak occurred at above 200 ^{o}C which was as a result of decomposition of MIL-53(Fe) to amorphous Fe_2O_3, the degradation of the organic ligand as seen in MIL-53(Fe) and also the degradation of the organic substances in the cow bone.

3.3 Analysis of samples

Table 2 shows the results for ultimate and proximate analysis of all samples as well as specific surface area and pore parameters of the samples. The prepared cow

bone char has a high surface area of 108.2 m^2 g^{-1}compared to that of MIL-53(Fe) with 69.5 m^2g^{-1}, while the composite recorded 125.6 m^2 g^{-1}. In terms of pore size, the synthesized MIL-53(Fe) has a higher value of 13.9 nm compared to that of cow bone char of 8.94 nm which explains the network structure of MIL-53(Fe) as highly flexible and opens up its pores to guest host (breathing effect), though having a small surface area compared to other metals (Janiak and Jana, 2010; Oladipo, 2018). And on introduction of cow bone char to the composite structure, there was a reduction in the pore size to 11.2 nm. The results obtained confirm that the composite have mesoporous structures suitable for the entrapment of the reactive species, chromium and subsequent enhancement of the adsorption process reactive species (Oladipo, 2018).

The elemental analysis indicates the presence of P_2O_5 higher in cow bone char than in the MIL-53(Fe)/cow bone char composite having 38.66% and 22.78% respectively with an absence in MIL-53(Fe) structure. This result is depicted on the SEM-EDX analysis of the samples. The percentage content of Iron (Fe) is seen to be higher in MIL-53(Fe) with 8.16% and MIL-53(Fe)/bone char composite with 8.23% compared to bone char having 0.07% of Fe.

Table 2: Properties of Samples

Property	**Cowbone char**	**MIL-53(Fe)**	**MIL-53(Fe)/Char**
Total surface area (m^2 g^{-1})	108.2	69.5	125.6
Pore size (nm)	8.94	13.9	11.2
Total pore volume (cm^3 g^{-1})	0.589	0.789	0.981
Micropore volume (cm^3 g^{-1})	0.237	0.396	0.325
Density (g cm^{-3})	0.69	0.89	1.12
Carbon content (%)	13	15.3	22.4
pHpzc (zero point charge)	6.7	4.5	5.4
P_2O_5 (%)	38.66		22.78
N_2 (%)	0.89		0.32
Fe (%)	0.07	8.16	8.23
Ca (%)	26.55		11.89
Mg (%)	0.67		0.23
SO_4 (%)	0.89		0.23
S(%)	0.38		0.004
Cation exchange capacity (meq g^{-1})	7.5	4.56	6.56

3.4 Adsorption column studies

3.4.1 Effect of time of collection

The contact time was determined for different flow rates of 5 ml/min and 15ml/min as shown in Fig. 9 & 10. The percentage removal of chromium increased up to 4 minutes having a maximum removal at 87.9% and 80.94% respectively following a reduction up to 14 minutes and there after no further changes was observed.

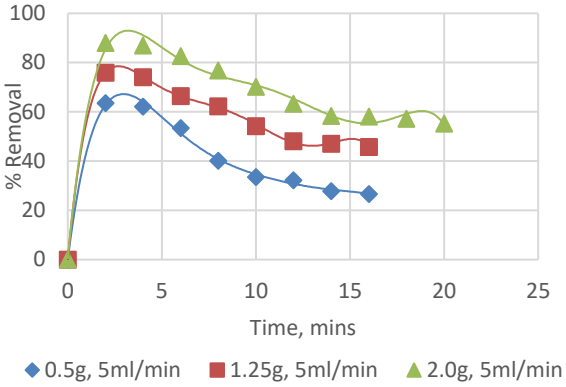

Fig. 9: Chromium removal with time (5ml/min)

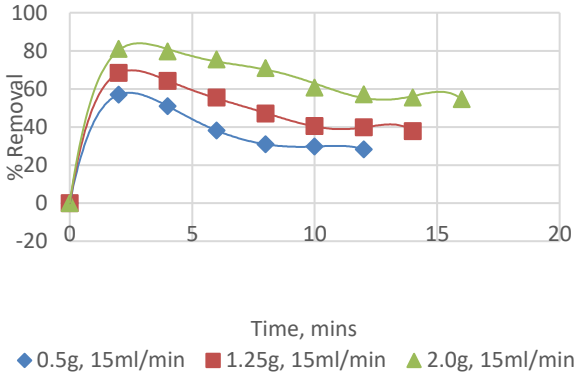

Fig.10: Chromium removal with time (15ml/min)

3.4.2 Effect of flow rate on breakthrough curve

The breakthrough curve in Figure 11 showed that at lower flow rate of 5ml/min, the surface of the composite was readily available for adsorption and more molecules were adsorbed as there was sufficient contact time with chromium molecules. Thus, having a higher adsorption percentage as well as a shallow adsorption zone and breakthrough and exhaustion were not quickly reached. While at higher flow rate, there was an increase in rate of mass transfer, shorter contact time and a steeper curve with relatively early breakthrough and exhaustion time which resulted in less adsorption uptake was observed. The observations drawn is in agreement with those reported by (Ghribi and Chlendi, 2011; Chowdhury *et al*., 2013; 2015; Dutta and Basu, 2014).

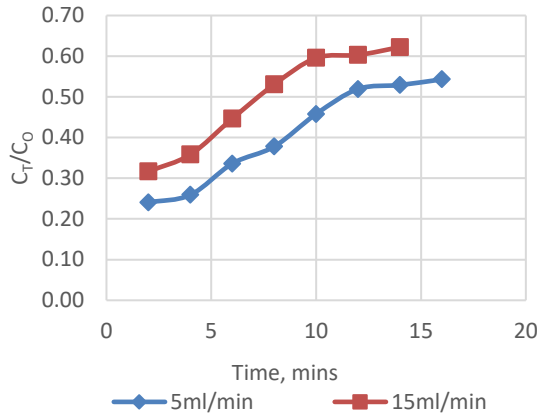

Fig.11: Breakthrough curve for chromium removal

3.4.2 Effect of bed height on chromium adsorption

Figure 12 shows the effect of bed height on chromium adsorption obtained for three different bed depths of 0.6 cm, 1.5 cm and 2.4 cm at 5 ml/min with an inlet concentration of 40 mg/l. A higher uptake was observed at a higher bed height of 2.4cm, as more adsorbate was passed down the bed, the adsorbent bed became saturated at which there was a reduction in the individual bed efficiency to about 58%. This observation is in agreement with those reported by (Ghribi and Chlendi, 2011; Chowdhury *et al*., 2013; 2015).

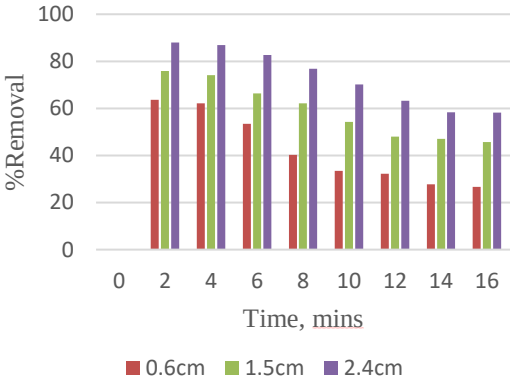

Fig.12: Bed height effect on adsorption of chromium

3.4.4 Equilibrium adsorption isotherm study

Table 3 and 4, the determination of coefficients (R^2) of the linear form of Langmuir model turned out to be satisfactory having an R^2> 0.9893 and 0.9933 respectively at a bed height of 2.4 cm.

Also, the maximum monolayer adsorption capacity of 19.61 mg/g was found at this same bed height of 2.4 cm compared to other bed heights which indicate uniform monolayer coverage. $R_L$values determined were found to be in the range $0<R_L<1$ which explains that the chromium ions is favorably adsorbed and the values of the equilibrium constant K_L were lower than unity which quantitatively reflects the strong affinity between the chromium ions and the MIL-53(Fe)/cow bone char composite.

K_F was determined to be 13.5515 mg/g, 6.63461 mg/g and 4.8759 mg/g which explains the random distribution of cow bone char between the crystallites of MIL-53(Fe) which may introduce heterogeneity onto the surface (Ghanizadeh *et al*., 2012) and a favorable sorption capacity.

From the Temkin plot, the heat of adsorption of chromium ions onto the composite was seen to be higher at 0.6 cm and reduced at 1.5 cm with a slight increase at 2.4 cm for both flow rates indicating an exothermic process. Also, the b values are lower than 80 kJ/mol which indicates that the adsorption of chromium ions onto MIL-53(Fe)/cow bone char composite is a physical adsorption process and consistent with FTIR analysis.

The mean energy of adsorption for chromium onto MIL-53(Fe)/cow bone char composite were all below 8 kJ/mol with R^2 values all at 0.9 and demonstrates that the adsorption of chromium onto MIL-53(Fe)/cow bone char is physisorption and plays an important role.

Table 3: Isotherm parameters for chromium adsorption onto MIL-53(Fe)/CBC composite

Isotherm	Adsorption Parameters, 0.6cm, 5ml/min	Adsorption Parameters, 1.5cm, 5ml/min	Adsorption Parameters, 2.4cm, 5ml/min
Langmuir	Q_m=4.2753mg/g K_L=0.087L/mg R_L= 0.22273 R^2=0.9579	Q_m=8.326mg/g K_L=0.170L/mg R_L= 0.12807 R^2=0.9850	Q_m=19.61mg/g K_L=0.368L/mg R_L=0.06361 R^2=0.9893
Freundlich	K_F=13.5515 1/n=1.20 n=0.830 R^2=0.9696	K_F=6.63461 1/n=0.62 n=1.596 R^2=0.9735	K_F=4.8759mg/g 1/n=0.35 n=2.824 R^2= 0.9608
Temkin	A_T=49.9198L/g b_T=196.586 B=12.603J/mol R^2= 0.9942	A_T=75.8987L/g b_T=275.601 B=8.9897J/mol R^2= 0.9896	A_T=174.354L/g b_T=246.206 B=10.063J/mol R^2= 0.978
Dubinin-Radushkevich	β=0.00004 Q_m=5.5384mg/g E=111.8J/mol R^2=0.9056	β=0.00001 Q_m=10.4093mg/g E=223.6J/mol R^2=0.8805	β=0.000002 Q_m=14.0202mg/g E=500J/mol R^2=0.8019

3.4.5 Kinetics of adsorption

Three kinetic models were employed to describe the sorption rates for chromium and obtained results are presented in Table 5.

Table 4: Isotherm parameters for chromium adsorption onto MIL-53(Fe)/CBC composite

Isotherm	Adsorption Parameters, 0.6cm, 15ml/min	Adsorption Parameters, 1.5cm, 15ml/min	Adsorption Parameters, 2.4cm, 15ml/min
Langmuir	Q_m=3.88048mg/g K_L=0.074L/mg R_L= 0.25306 R^2=0.9767	Q_m=6.21891 mg/g K_L=0.116L/mg R_L= 0.17683 R^2=0.9811	Q_m=17.67mg/g K_L=0.259L/mg R_L= 0.08792 R^2=0.9933
Freundlich	K_F=17.374mg/g 1/n=1.37 n=0.726 R^2=0.9829	K_F=9.053mg/g 1/n=0.88 n=1.135 R^2=0.9782	K_F=6.857mg/g 1/n=0.46 n=2.183 R^2= 0.9818
Temkin	A_T=47.7674L/g b_T=182.55 B=13.572J/mol R^2= 0.9969	A_T=58.1506L/g b_T=226.345 B=10.946J/mol R^2= 0.9937	A_T=110.757L/g b_T=201.691 B=12.284J/mol R^2= 0.9910
Dubinin-Radushkevich	β=0.00006 Q_m=4.8105mg/g E=91.2871J/mol R^2=0.9446	β=0.00002 Q_m=7.87505 mg/g E=158.114J/mol R^2=0.9133	β=0.000005 Q_m=12.59mg/g E=316.228J/mol R^2=0.9011

The equilibrium adsorption of chromium onto MIL-53(Fe)/cow bone char composite could be best described with the pseudo-second order kinetic model judging by the R^2 values depicted in Table 5.

Table 5: Kinetic model parameters for chromium adsorption onto MIL- 53(Fe)/CBC composite.

Model	Kinetic parameters
Lagergren Pseudo First-order	k_1 (min^{-1})= 0.2096 q_1 (mg/g)=14.047 R^2=0.963
Pseudo second-order	k_2 ($gmg^{-1}min^{-1}$) =0.04304 q_2 (mg/g)=12.3762 R^2=0.9911
Intraparticle diffusion	k_{ad}($mgg^{-1}min^{-1(1/2)}$ =3.0312 C_i(mg/g)=26.353 R^2=0.9503

CONCLUSIONS

In the present work, MIL-53(Fe)/Cow bone charcoal composite, was successfully prepared via the sol-gel method and was tested for the removal of chromium from real tannery effluent. The adsorption process was found to be efficient below the pH_{pzc} of 5.4. The kinetic studies showed that the adsorption data were fitted well to the pseudo second-order model with high correlation coefficient R^2=0.9911. The adsorption isotherm equilibrium studies confirmed that the Langmuir model best described the adsorption process of chromium onto MIL-53(Fe)/Cow bone char composite. Adsorption capacity of MIL-53(Fe)/Cow bone char composite for chromium was 19.61mg/g with a removal efficiency of 87.8% at an optimal bed height of 2.4cm (2.0g) for MIL-53(Fe)/Cow bone char composite. A result from analysis of data with Dubinin–Radushkevich and Temkin isotherms showed that adsorption of chromium onto MIL-53(Fe)/Cow bone char composite is physical in nature.

REFERENCES

Agoyi O.R., Igboro S.B., Okuofo C.A. (2015). *Performance of Cow bone Char in Fixed-Bed Column for the Treatment of Industrial Wastewater*. Kaduna State: Department of Water Resources and Environmental Engineering, Ahmadu Bello University, Zaria.

Araoye, B. O. (2015). A Study of the Development, Characterisation and Degradability of Polyester/Nano-Locust Bean Pods Ash Composite. Ahmadu Bello University, Zaria, Department of Metallurgical and Materials Engineering.

Chowdhury, T, L. Zhang , J. Zhang and S. Aggarwal. (2018). Removal of Arsenic(III) from Aqueous Solution Using Metal Organic Framework-Graphene Oxide Nanocomposite. *Nanomaterials (8)*, 1-18.

Chowdhury, Z. Z., Zain,S.M., Rashid,A. K., Rafique,R. F., & Khalid, K. (2013). Breakthrough Curve Analysis for Column Dynamics Sorption of Mn(II) Ions from Wastewater by Using Mangostana garcinia Peel-Based Granular-Activated Carbon. *Journal of Chemistry*, 1-8. doi:http://dx.doi.org/10.1155/2013/959761

Fawell, J. (2006). Fluoride in drinking-water (1st published. ed.). *WHO ISBN 9241563192.*, 47.

Ghader Ghanizadeh, Ghorban Asgari, Abdol Motaleb Seid Mohammadi and Mohammad Taghi Ghaneian. (2012). Kinetics and Isotherm Studies of Hexavalent Chromium Adsorption from Water using Bone Charcoal. *Fresenius Environmental Bulletin*, 1296-1302.

Janiak, C and Jana K. V.. (2010),. MOFs, MILs and more: concepts, properties and applications for porous coordination networks (PCNs). *New Journal of Chemistry, 34*, Pages 2337–2684. Retrieved from www.rsc.org/njc

Oke,I. A., Otun, J. A., Okuofu,C. A. and Olarinoye,N. O. (2006). Characteristics of Tanning Industries in Nigeria for Aquatic Animals and Plants. *Research Journal of Agriculture and Biological Sciences, 2(5)*, 209-217.

Oladipo, A. A. (2018). MIL-53 (Fe)-based photo-sensitive composite for degradation of organochlorinated herbicide and enhanced reduction of Cr(VI). *Process Safety and Environmental Protection (116)*, 413-423.

Mohammed, SSD; Orukotan, AA; Abdullahi, H. (2017). Physicochemical and Bacteriological Assessment of Tannery Effluent from Samaru-Zaria, Kaduna State, Nigeria. *Journal of Applied Science and Environmental Management (4), 21*, 734-740. doi:10.4314/jasem.v21i4.14